Int. J. Heat Mass Transfer. Vol. 35, No. 4, pp. 847–860, 1992
Printed in Great Britain

0017–9310/92 $5.00 + 0.00

Heat transfer in the splash zone of a bubbling fluidized bed

A. DYRNESS, L. R. GLICKSMAN and T. YULE
Department of Mechanical Engineering, Massachusetts Institute of Technology, Cambridge, MA 02139, U.S.A.

(*Received* 1 *November* 1988 *and in final form* 22 *April* 1991)

Abstract—The heat transfer in the splash zone of a bubbling fluidized bed is measured for six different geometries of horizontal tube bundles over a range of superficial velocities. The heat transfer decreases exponentially with vertical distance above the expanded bed surface. The results are correlated by use of a nondimensional vertical distance $XU_{mf}/L(U-U_{mf})$ where L is the horizontal pitch of tubes in a staggered array. The same correlation gives reasonable agreement with other data reported in the literature taken for large particle bubbling beds. The splash zone heat transfer is proportional to the measured local particle density in the splash zone.

INTRODUCTION

ONE PROPOSED method to control the off-design capacity of a bubbling fluidized bed combustor is to place horizontal tubes near the upper bed surface. As the superficial gas velocity is reduced the bed surface will drop, uncovering some tubes in the splash zone where the heat transfer to the tubes should be reduced. In order to properly design such a system, the heat transfer in the splash zone must be clearly understood. In this paper, recent experimental results will be presented along with a general correlation for splash zone heat transfer.

Past work

There have been numerous studies of heat transfer to horizontal tubes within the dense phase of a fluidized bed. In contrast, there are only a handful of studies of the heat transfer in the splash zone of a fluidized bed. George and Grace [1] carried out an experimental study using a tube bundle with four vertical rows of tubes. They also proposed a correlation for the heat transfer coefficient as a function of distance above the expanded bed surface scaled to the transport disengaging height. They demonstrated that data of other investigations followed a similar form; but they used empirical results of the other investigations to establish the scaling dimension.

Byam *et al.* [2] measured experimental heat transfer data in the freeboard of a hot, pressurized fluidized bed combustor. The form of the variation with height is similar to that found by George and Grace [1]. Kortleven *et al.* [3] measured the heat transfer in the splash zone of an atmospheric fluidized bed combustor over a wide range of superficial velocities. Xavier and Davidson [4] made heat transfer measurements in the freeboard of a slugging bed at ambient conditions. Biyikli *et al.* [5] made measurements on a single tube in the freeboard of an open bed at ambient conditions; they did not report the flow conditions, but by Stewart's criteria the bed was slugging. Wood *et al.* [6] also presented data for horizontal tube banks in the splash zone of a bed at ambient conditions.

The general trend of the heat transfer decrease with distance above the expanded bed surface has been established by the experimental studies reported in the literature. However, the length scaling factor, controlling the rate of decrease of the heat transfer with vertical distance from the bed surface cannot be confidently predicted.

In the present paper experimental heat transfer measurements made in the splash zone of an ambient model of a bubbling fluidized bed combustor are reported for six different in-bed tube geometries. A generalized correlation is also developed and compared to a wide range of data.

EXPERIMENTAL

Fluidized bed facility

The atmospheric fluidized bed facility at MIT is an ambient temperature and pressure scale model of a 20 MW pilot plant operated by the Tennessee Valley Authority (TVA). In accordance with the scaling laws derived and verified by Nicastro and Glicksman [7] and Glicksman [8] the hydrodynamics of a hot bed can be reproduced in a properly scaled bed at ambient conditions. In scaling the bed operation, the Reynolds number, the Froude number, the solid to gas density ratio, and the non-dimensional particle size distribution are kept identical between the 20 MW combustor and the model. To achieve equal value of the dimensionless parameters the scaled bed uses steel grit particles with a density 3.5 times larger than the hot bed particles. All linear dimensions in the cold bed are reduced by a factor of 4 and the velocity is halved.

NOMENCLATURE

d_i	particle diameter	v_{p0}	particle velocity
d_p	mean particle diameter	x	vertical distance above expanded bed surface
D_T	tube diameter	x_i	weight fraction
F_D	drag force per unit volume	x_{MAX}	maximum vertical distance
h	heat transfer coefficient	$\bar{x}$	characteristic vertical length for splash zone heat transfer.
h_∞	heat transfer coefficient high in the freeboard		
h_b	heat transfer coefficient with dense bed		
H_{b0}	bed depth at minimum fluidization	Greek symbols	
L	characteristic system length	ε_{mf}	voidage at minimum fluidization
L_T	tube length	ε_Γ	voidage at surface of tube
U	superficial velocity	ρ_0	density in freeboard
U_c	gas velocity in cavity	ρ_{mf}	density in dense bed at U_{mf}
U_{mf}	minimum fluidization velocity	ρ_p	density of a single particle.

The cold bed has a cross-section of 89 cm by 107 cm which forms a model of approximately two-thirds of the cross-section of the TVA 20 MW plant [9].

Heat exchanger configuration

A total of six different horizontal tube bundle geometries were examined. The reference geometry is the initial tube bundle used in the TVA 20 MW pilot plant. All of the other geometries can be described in reference to the 20 MW geometry. Table 1 lists the geometric characteristics of all six tube banks; these are illustrated in Figs. 1–6. In the MIT facility, all lengths are scaled down by a factor of four, and all velocities are reduced by a factor of two. The reference cold bed geometry has staggered rows of tubes with horizontal and vertical center pitch of 1.9 cm, which corresponds to 6.7 cm in the TVA pilot plant.

In practice, heat exchangers are installed in fluidized bed combustors with some adjacent columns of tubes removed to allow access for repairs or scheduled maintenance. The Lanes geometry was designed to investigate the effect of missing adjacent columns. The Lanes geometry is identical to the 20 MW geometry except that two columns in four locations have been removed. All of the geometries under investigation have staggered rows except the Sparse geometry. The Sparse geometry is the same as the 20 MW geometry except that every other column has been removed, resulting in a square pattern.

There exists some uncertainty in the literature as to the importance of horizontal and vertical pitch in determining the hydrodynamic behavior in fluidized beds. The Horizontally Compact geometry, has the same vertical pitch as the 20 MW geometry, and a horizontal pitch reduced by 16.6% relative to the 20 MW geometry. To keep the number of tubes the same as in the 20 MW geometry, three tubes per column were installed. The Vertically Compact geometry, while having the same horizontal pitch as the 20 MW geometry, has a vertical pitch of 1.37 cm, a reduction of 28% relative to the 20 MW geometry. The Vertically Expanded geometry has the same horizontal

Table 1. Geometric characteristics of the tube bundles (all dimensions given in centimeters followed by dimension in inches)

Geometry name	D_b (cm)	Horizontal pitch (cm)	Vertical pitch (cm)	Tube bundle height	Geometric arrangement
Original	3.81 (1.5)	1.9 (0.75)	1.9 (0.75)	15.9 (6.25)	Staggered
Lanes[a]	[a]	1.9 (0.75)	1.9 (0.75)	15.9 (6.25)	Staggered w/ in line lanes
Sparse	5.4 (2.12)	3.81 (1.50)	3.81 (1.50)	11.43 (4.50)	In line
Horizontally compact	3.49 (1.375)	1.59 (0.625)	1.9 (0.75)	9.52 (3.75)	Staggered
Vertically compact	3.62 (1.285)	1.9 (0.75)	1.37 (0.54)	12.29 (4.82)	Staggered
Vertically expanded	5.4 (2.125)	1.9 (0.75)	3.49 (1.375)	11.43 (4.50)	Staggered

[a]See Fig. 3.

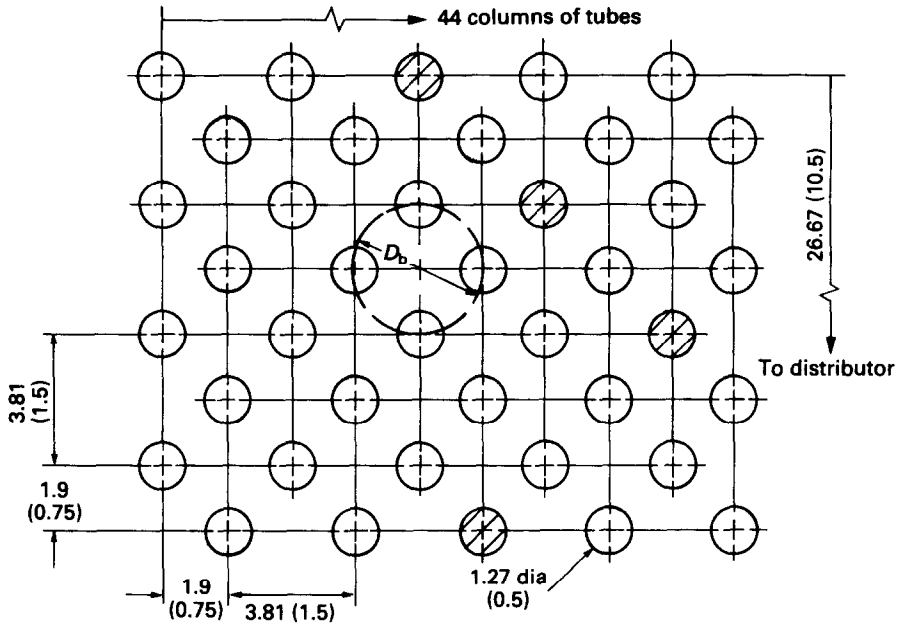

FIG. 1. Original tube bundle configuration. D_b is the average bubble diameter. Tubes used for heat transfer measurements are cross-hatched in the figure. Units in cm (in.)

pitch as the 20 MW geometry, and its vertical pitch is increased by 83.3% relative to the 20 MW geometry.

All of the tubes were constructed of 1.27 cm diameter copper tubes 89 cm long. The correct spacing of each tube bundle was established by using 1.91 cm thick plywood template guides to hold the ends of the tubes. The tube bundles covered the entire bed area to provide uniform fluidization.

Heat transfer measurements

Aluminum tubes containing electric heaters are used to measure the heat transfer coefficients at various locations in the bundle. The heater locations are designated by cross hatching in Figs. 1–6. The instrumented heat transfer tube has a 0.64 cm diameter heater inserted into the 1.27 cm aluminum tube. The ends of the heaters are insulated with PVC or Teflon

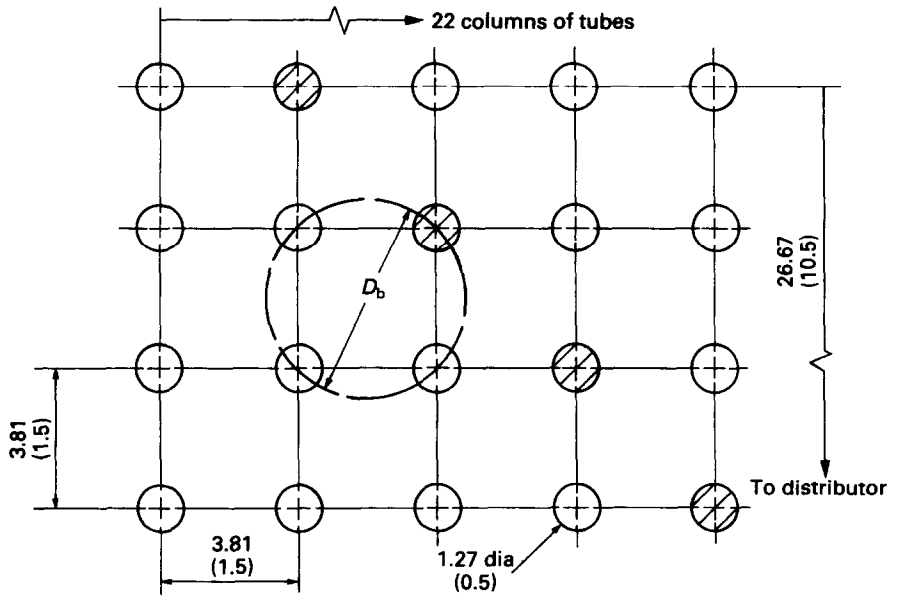

FIG. 2. Sparse tube bundle configuration. Average bubble diameter for lanes, D_b = 5.39 cm.

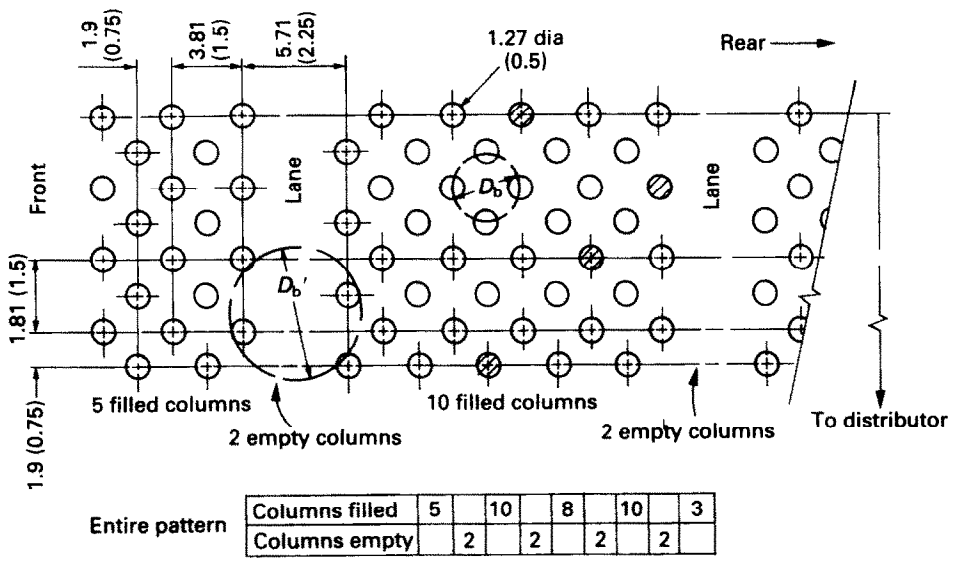

FIG. 3. Lanes tube bundle configuration. Units cm (in.). Average bubble diameter for tubes, $D_b = 3.81$ cm (1.5 in.). Average bubble diameter for lanes, $D_b = 7.04$ cm (2.77 in.).

2.5 cm long. A groove has been milled on the exterior of the tube; a thermocouple is bonded in the groove to measure the tube temperature. A thermocouple was placed in the dense phase of the bed to monitor the bed temperature. The heat transfer coefficient was found from an energy balance; the maximum uncertainty in h due to uncertainties in the measured temperature and heat flux is estimated to be 10%. This has been confirmed by measurements in single phase air streams on prototypes of these heaters. Distances are measured in the freeboard from the time-averaged surface of the bubbling bed as determined from extrapolation of static pressure measurements in the dense bed.

Particle size distribution

The particle size distribution was determined by weighing particles, sized using standard sieves. The average particle diameter based on surface area is determined by $[1/(\Sigma x_i/d_i)]$. The material used in the MIT facility is iron grit that has a sphericity of approximately 0.80 and a static density of 8097 kg

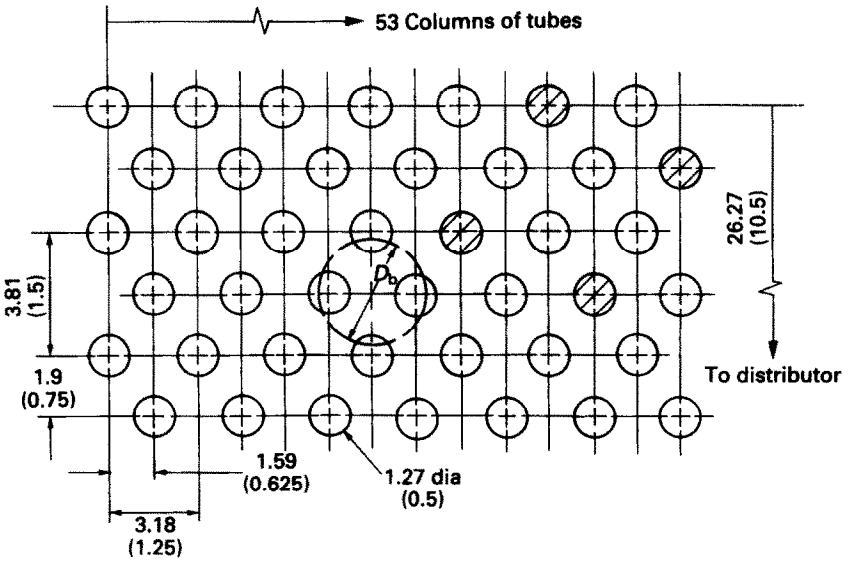

FIG. 4. Horizontally compact tube bundle configuration. Units cm (in.). Average bubble diameter, $D_b = 3.49$ cm (1.375 in.).

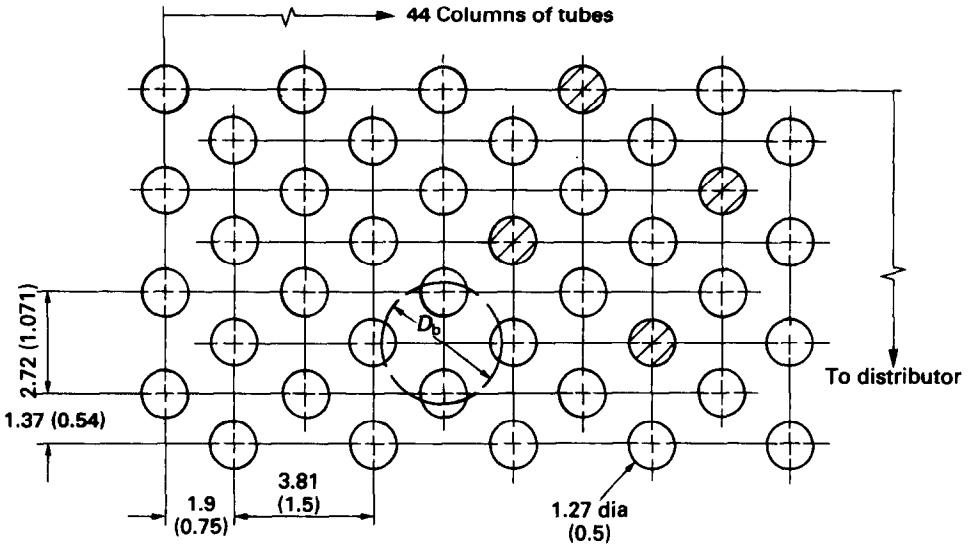

FIG. 5. Vertically compact tube bundle configuration. Units cm (in.). Average bubble diameter, D_b = 3.26 cm (1.285 in.).

m^{-3} [9]. To keep the particle size distribution constant, fine particles are captured by cyclones in the exhaust and fed by gravity to a hopper next to the bed. From the hopper, particles are pneumatically reinjected into the dense phase of the fluidized bed. Dryers have been installed in the injection air supply line to remove excess moisture. Two particle size distributions of the steel grit were used, with and without fines reinjection. The mean diameters are 0.250 and 0.200 mm with minimum fluidization velocities of 0.15 and 0.12 m s^{-1}, respectively.

Analysis

For this work attention will be limited to the splash zone of a bed containing large particles. These particles are thrown upward by means of bubble eruptions at the bed surface. The large particles will, to a first approximation, follow a ballistic trajectory. The

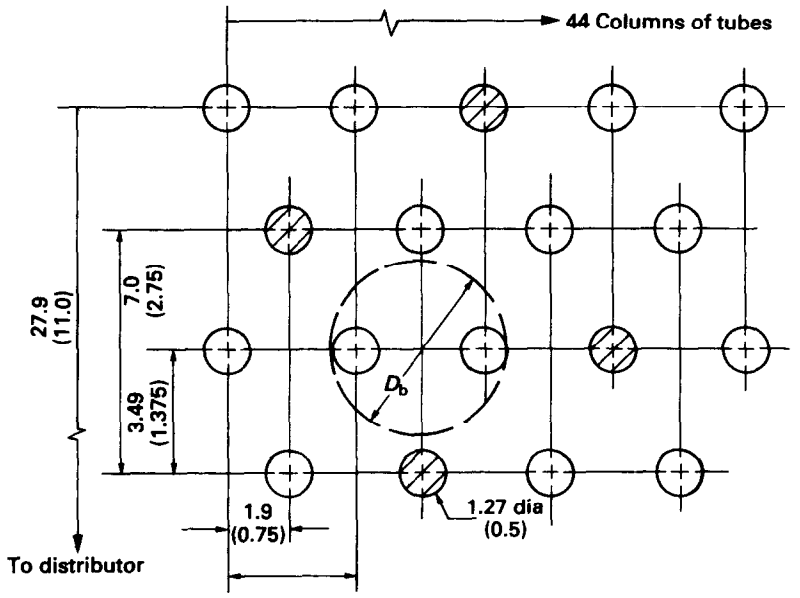

FIG. 6. Vertically expanded tube bundle configuration. Units cm (in.). Average bubble diameter, D_b = 5.4 cm (2.125 in.).

maximum height they will achieve above the bed surface is related to their velocity as they leave the bed surface

$$x_{max} = \frac{v_{p0}^2}{2g}. \quad (1)$$

The heat transfer in the freeboard should be proportional to the local density of particles in the freeboard. Following the early work by Lewis *et al.* [10] as well as recent results by Piper [11] for the same steel grit particles used in the present experiment, the density should decrease exponentially with the distance above the expanded bed surface. The distance should be scaled with x_{max}. Thus the expected form of the splash zone heat transfer coefficient should be

$$h \sim \exp\left(-\frac{cx}{x_{max}}\right). \quad (2)$$

Experiments on large particle bubbling beds have shown that only about 20% of the gas flow in excess of minimum fluidization passes through the bed by upward motion of visible bubbles or cavities. The majority of the excess gas flows through channels or voids at the surface of the bed formed by single or multiple coalescing bubbles at the surface [12]. The velocities through these channels may be in excess of $10U_{mf}$. The high gas velocity accelerates the layer of particles between adjacent vertical coalescing bubbles. Levy *et al.* [13] have shown that the accelerating particles remain in clustered layers until they pass the upper bed surface. The resulting particle velocities must be well in excess of the rise velocity of bubbles to account for the observed particle trajectory in the splash zone [9]; the particle velocities must also be greater than the bubble rise velocity to account for the height within the splash zone in which horizontal tubes exhibit heat transfer augmentation.

A simplified model to establish the functional relationships between v_{p0} and x_{max} will be developed for large particles. The gas flow through the bubble cavity, U_c, is taken to be a constant. Writing the equation of motion in the vertical direction for particles within the cavity

$$\rho_p \frac{\pi d_p^3}{6} \frac{dv_p}{dt} = F_D \frac{\pi d_p^3}{6} \quad (3)$$

where F_D is the drag force of the gas per unit volume of the particle. Since U_c is much larger than U_{mf} the gravity term is omitted from equation (3). Linearizing the drag term† it follows from the minimum fluidization condition that if the particles remain clustered together

$$F_D = \rho_p g \frac{U_c}{U_{mf}}. \quad (4)$$

Rewriting equation (3)

$$\rho_p \frac{dv_p}{dt} = \rho_p v_p \frac{dv_p}{dx} = \rho_p g \frac{U_c}{U_{mf}} \quad (5)$$

where it is further noted that $U_c \gg v_p$. Then solving for v_{p0} when the particles have moved a distance L

$$\frac{v_{p0}^2}{2} \approx g \frac{U_c}{U_{mf}} L \quad (6)$$

where L is the cavity length which should be some multiple (two or three at most) of the bubble diameter. For a bed with a substantial number of tube rows below the expanded bed height, the bubble diameter is in turn related to the tube spacing. Thus, L should be proportional to the tube spacing. From equation (1)

$$x_{max} = \frac{v_{p0}^2}{2g} \approx L \frac{U_c}{U_{mf}}. \quad (7)$$

Since most of the excess gas flow passes through the bubble cavity at the surface of the bed, U_c should be proportional to $(U - U_{mf})$ divided by the average bubble voidage at the bed surface. Thus, the form x_{max} should follow is

$$x_{max} \sim L \frac{(U - U_{mf})}{U_{mf}} \quad (8)$$

and using the form of equation (2)

$$h \approx h_b \exp\left[-\frac{cx}{L\left(\frac{U}{U_{mf}} - 1\right)}\right] \quad (9)$$

where the origin of x is the location of the expanded bed surface and h_b the heat transfer coefficient in the dense bed. When the heat transfer coefficient in the freeboard far above the splash zone, h_∞, is significant an alternate form is suggested

$$h - h_\infty \approx (h_b - h_\infty) \exp\left[-\frac{cx}{L\left(\frac{U}{U_{mf}} - 1\right)}\right]. \quad (10)$$

The form of equation (10) indicates that the heat transfer coefficient in the splash zone is a function of three factors, the vertical distance above the expanded bed surface, the horizontal tube spacing, and the superficial gas velocity.

The experimental data of the present work will be used to estimate the constant c; the present data as well as data in the literature will be compared with equations (9) and (10). It must be mentioned that the form of the equations derived are based on a simple model of the process for large particles. A more exact prediction will require a detailed model of the particle behavior during bubble eruption.

† For the mean particle sizes used in this study the linear resistance term in the Ergun equation is controlling for velocities up to at least $20U_{mf}$.

Particle loading in the splash zone

Particles moving over a horizontal tube in the splash zone at velocities of the order of v_{p0} will have a contact time at the tube surface of the magnitude of D_T/v_{p0}. When $v_{p0} \geq U_{mf}$ the transient time will be small compared to the thermal time constant of the individual particle. Thus, the particles will remain at approximately the bed temperature while they are adjacent to the tube surface. The heat transfer between the particles and the tube surface should be determined by the isothermal large particle model [14], once the average spacing of particles on the tube surface or alternatively the average surface voidage is known.

Consider particles with a velocity v_p moving toward the tube alternatively from above it and below it in the splash zone. In the splash zone at a distance x the average density of particles will be taken as ρ_0. If the particles are large they will be unable to follow the gas stream and avoid the tube surface. Thus, the particles in the projected area of the tube $D_T L_T$ will strike the tube. If the number is modest, these particles will form a single layer on the surface and follow the surface to the midpoint where they will leave the tube surface. The particles will be assumed to move over the tube surface with a velocity proportional to the tangential component of v, the free stream velocity. The surface voidage on the tube ε_T can be shown to be

$$\frac{1-\varepsilon_T}{1-\varepsilon_{mf}} = \frac{3}{4}\frac{\rho_0 D_T}{\rho_{mf} d_p} \tag{11}$$

where ρ_{mf} is the effective density of the bed at U_{mf} which has a voidage ε_{mf}. Thus to achieve surface particle packing $(1-\varepsilon_T)$ on a tube in the splash zone which approaches the magnitude of the packing in the dense phase, the splash zone density must be approximately $\rho_{mf}/d_p/D_T$. By the isothermal model the heat transfer coefficient should be proportional to $1-\varepsilon_T$ and this in turn is proportional to ρ_0. Heat transfer on the bare portion of the tube can be shown to be negligible. Interestingly, this model indicates that ρ_0 can be much less than ρ_{mf} and still achieve h close to h_b (note this condition for ρ_0 results in an average particle spacing to particle diameter of 5 in the freeboard away from the tube surface; still a very dense freeboard condition). Piper measured the density in the freeboard of a bed with tubes using the same particles used in the present study. He found an exponential decrease of density with distance above the bed surface.

RESULTS

Each tube bank geometry was tested with coarse and fine particle size distributions. For the coarse particle tests, heat transfer results were obtained for superficial velocities as high as 1.4 m s^{-1}. The limitations imposed by the fine particle reinjection system restricted the superficial velocities for this condition to less than 1.1 m s^{-1}.

Figure 7 shows heat transfer results for the original tube configuration. The vertical location of a particular instrumented tube is given in relationship to the expanded bed surface for that test condition. Figure 7 includes data obtained for U_0/U_{mf} between 2 and 8.2 and for three initial bed depths, measured when the bed is defluidized. The results, which are typical of those found for all of the cases, show that the heat transfer coefficient is essentially constant when the instrumented tube is beneath the expanded bed surface. As the tube is located higher in the splash zone above the expanded bed height, the heat transfer coefficient falls rapidly. There is also some modest decrease in the heat transfer coefficient when the tube is still in the dense bed but near the expanded bed

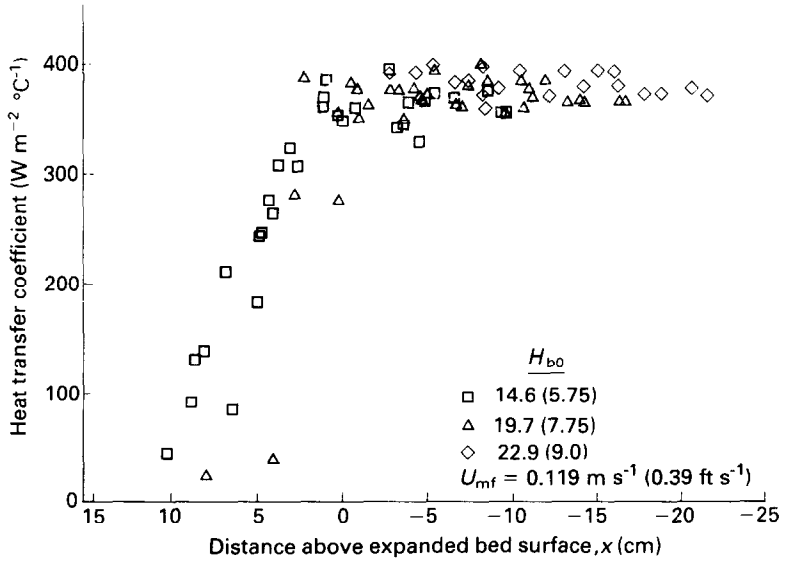

FIG. 7. Original tube configuration heat transfer performance with fines.

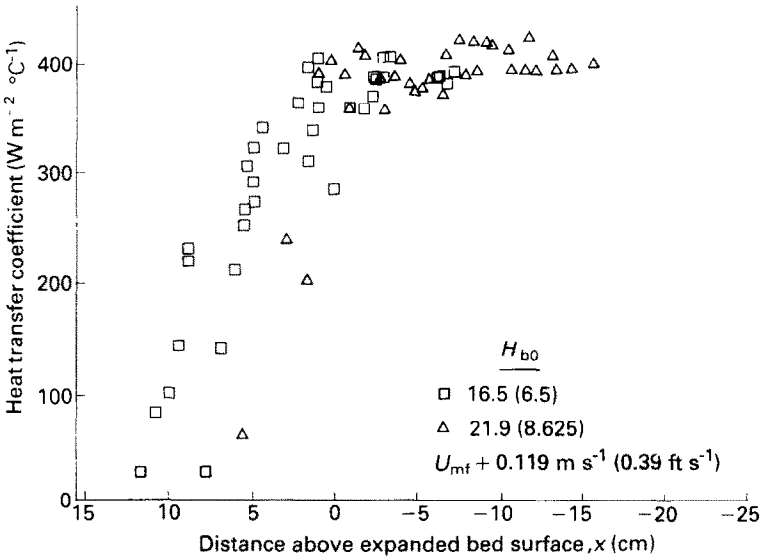

FIG. 8. Sparse heat transfer performance with fines.

surface. This may be due in part to the uncertainty in determining the location of the expanded bed surface. The data points shown on Fig. 7 in the splash zone correspond to a range of superficial gas velocities, the influence of this parameter will be more clearly seen in succeeding figures.

Figure 8 shows similar heat transfer results for the sparse tube geometry. The data scatter at high values of x is due in part to variation in U_0/U_{mf}. Figures 9–12 show the results for the following tube geometries: lanes, horizontally compact, vertically compact and vertically expanded, respectively. All of the results are for the particles which contain fines.

To generalize the heat transfer data, the form suggested by equation (9) of the analysis was adopted. For the results of the original geometry, shown on Fig. 7, the best fit is obtained when the constant $c = 1.5$

$$h = h_b \exp - \left[\frac{1.5xU_{mf}}{L(U-U_{mf})}\right] \tag{12}$$

where L, the characteristic system dimension, is equal to the horizontal pitch of a tube row. As shown in Fig. 1 the horizontal pitch for the 20 MW geometry is also equal to the maximum bubble size which can be constructed within the boundaries of adjacent tube centers.

This same correlation yields a good characterization for all of the experimental results. Figure 13 shows a generalized correlation of the data for the particle with fines reinjection and Fig. 14 shows similar results for the coarser particle distribution. For all staggered tube arrays the best fit is achieved when L is taken as the horizontal tube spacing. The results for the vertically expanded and vertically com-

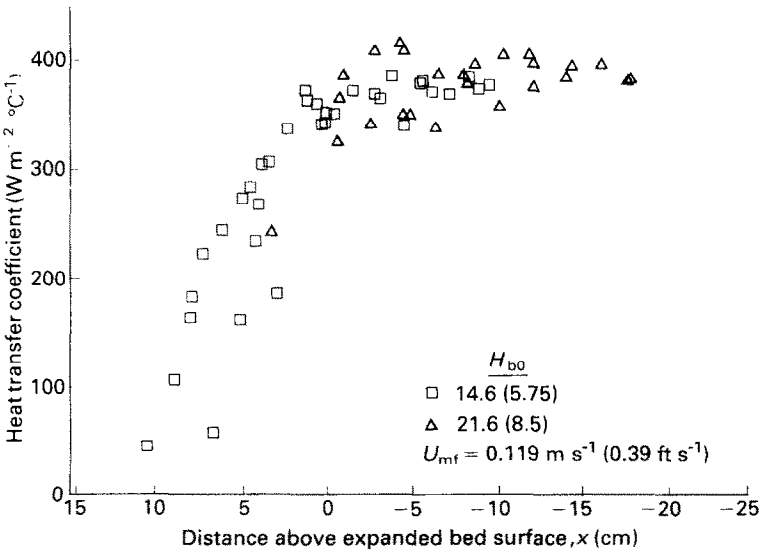

FIG. 9. Lanes heat transfer performance with fines.

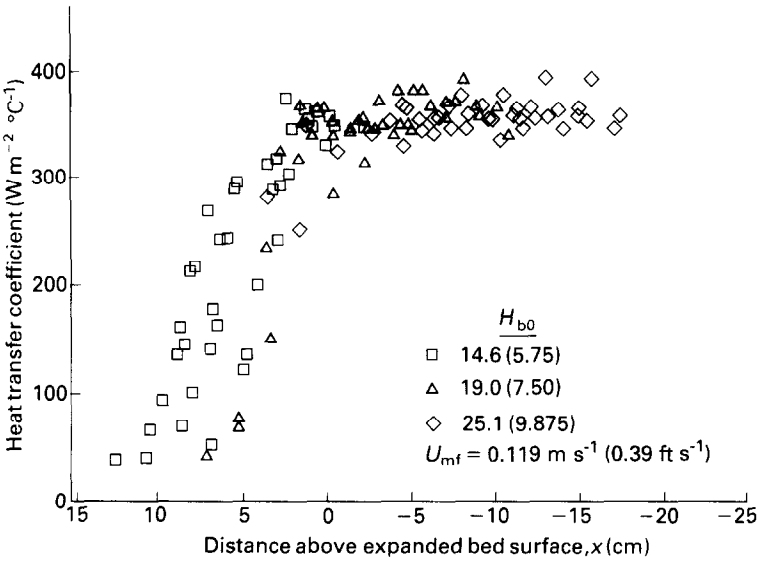

FIG. 10. Horizontally compact heat transfer performance with fines.

pact arrays show little influence of the vertical pitch on splash zone heat transfer. However, the degree of expansion was found to be influenced by the vertical tube pitch.

For the square tube array, the sparse geometry, the best correlation was achieved when L was set equal to the circumscribed bubble diameter shown in Fig. 2 rather than the horizontal tube pitch.

Figures 15–17 more explicitly illustrate the influence of superficial velocity at three fixed distances above the expanded bed surface. The data shown is taken from a combination of geometries tested with the fine particle distribution. The correlation gives a good representation of the trends due to superficial velocity. The correlation does not eliminate all of the scatter in the heat transfer results. Most of this can be traced to the scatter of the original data for a given tube geometry, expanded bed height, and superficial velocity. The scatter would probably be reduced if measurements were averaged over a larger number of different horizontal locations in the splash zone.

Figure 18 shows the particle density distributions measured in the freeboard of a bed with horizontal tubes by Piper. Also shown on the figure is a correlation of the data using the same form as equation (12). The close agreement indicates that the splash zone heat transfer is proportional to local particle density in the splash zone. Using the density correlation shown on Fig. 18 combined with equation (11), the particle density around the tube surface becomes

$$\frac{1-\varepsilon_T}{1-\varepsilon_{mf}} = 3.2 \exp - \left[\frac{1.5X}{L\left(\frac{U}{U_{mf}} - 1\right)} \right]. \qquad (13)$$

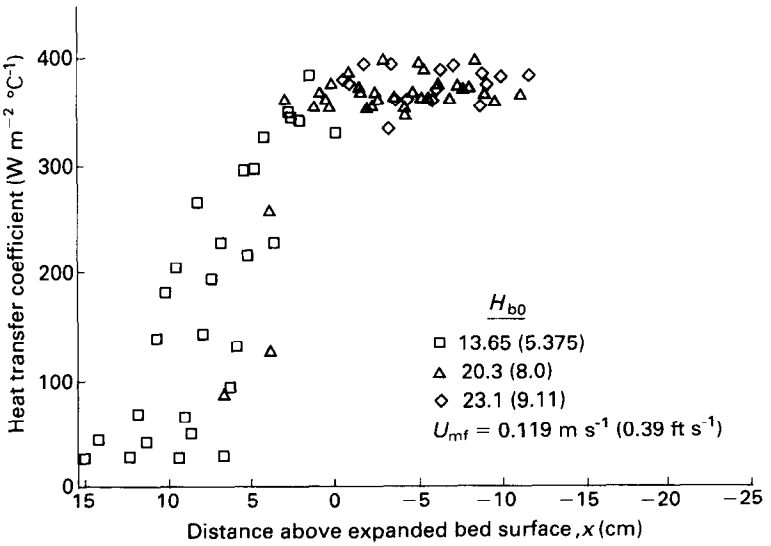

FIG. 11. Vertically compact heat transfer performance with fines.

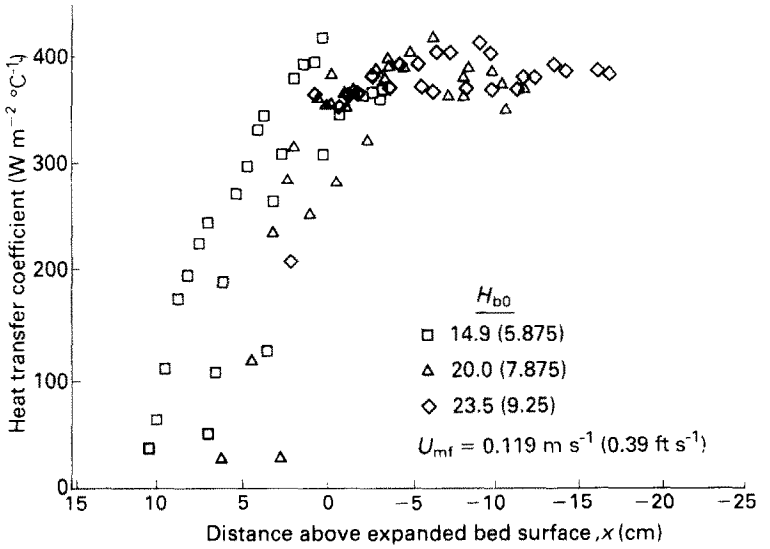

FIG. 12. Vertically expanded heat transfer performance with fines.

The ratio h/h_b should vary with the ratio of the solid fraction at the tube surface, $(1-\varepsilon_T):(1-\varepsilon_{mf})$. To achieve agreement with the measured values of h/h_b, the constant multiplying the exponential in equation (13) should be unity rather than 3.2. This is due to the simplifying assumptions used to derive equation (11), e.g. only a single layer of particles flow around the tube surface. The fact that the constant is of the order of magnitude unity confirms the close relationship between the particle density in the freeboard and the heat transfer coefficient in the freeboard.

Comparison to other work

Using the form of the expression derived earlier, equations (10) and (13), the exponent of equation (12) can be rewritten as

$$\frac{1.5X}{L\left(\dfrac{U}{U_{mf}}-1\right)} = x/\bar{x}. \tag{14}$$

The form of the results given by Byam *et al.* for a tube bank in the splash zone of a pressurized combustor as well as George and Grace's [1] results for a bed at ambient conditions clearly follow the form of equation (12). The linear scaling parameter x' defined by George and Grace [1] is approximately equivalent to $2.5\bar{x}$. When x' is estimated as $TDH/3.5$ as recommended by George and Grace [1], it overpredicts $\bar{x}$ for the present results by a factor of 4 or more.

Table 2 shows a comparison of equation (14) with other work in the literature. In each case an exponential function was fitted to the data to obtain the

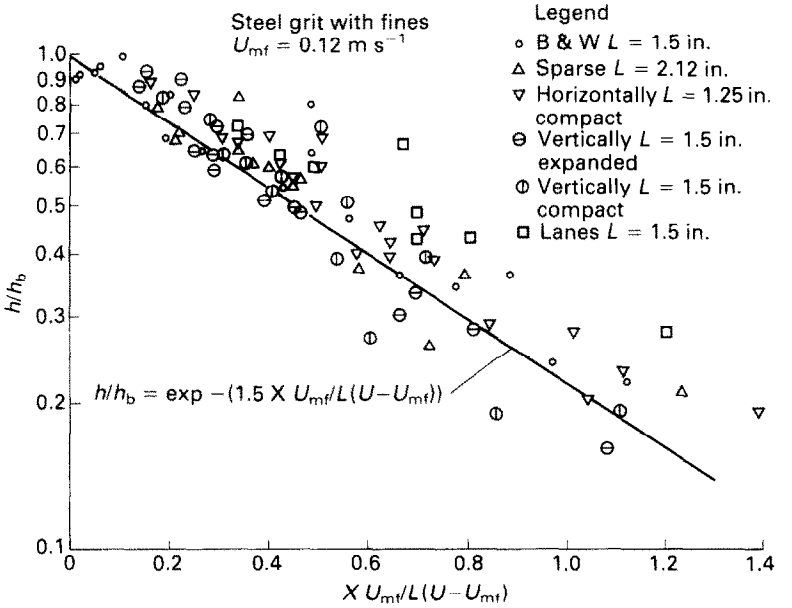

FIG. 13. Heat transfer in the splash zone with different tube bundle geometries. Steel grit with fines, $U_{mf} = 0.12$ m s^{-1}.

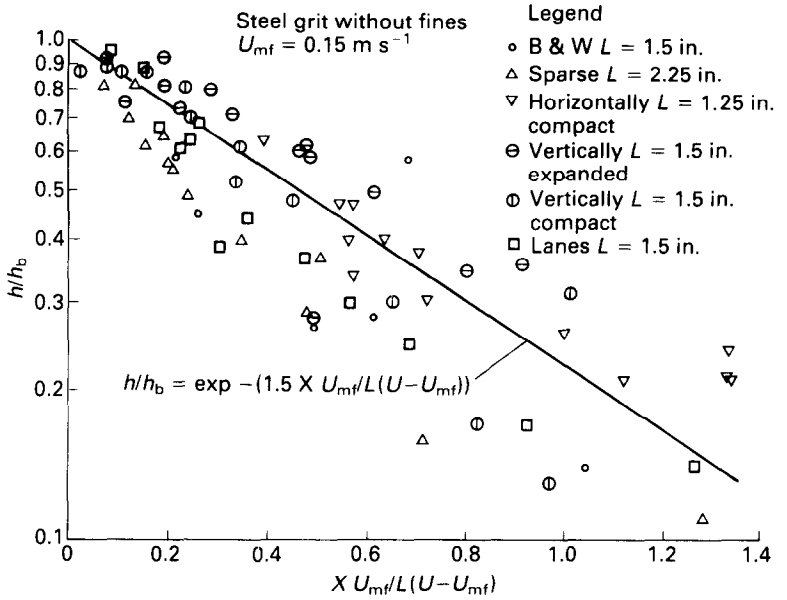

FIG. 14. Heat transfer in the splash zone with different tube bundle geometries. Steel grit without fines, $U_{mf} = 0.15$ m s^{-1}.

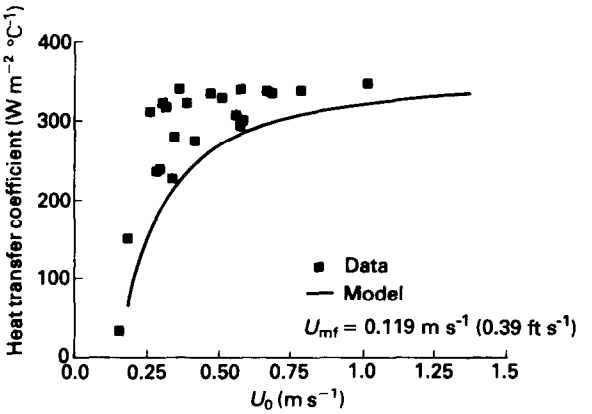

FIG. 15. Crossplot for relative bed height of 2.54 cm with fines.

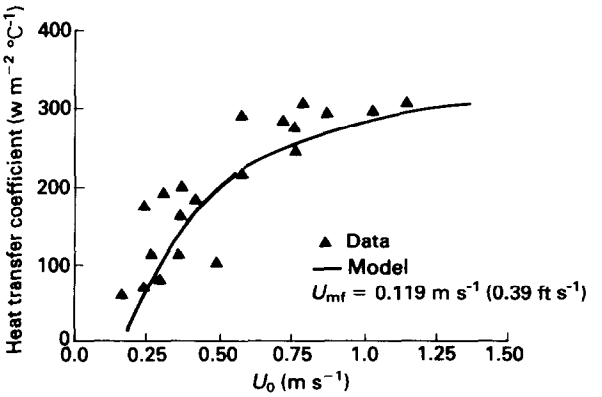

FIG. 16. Crossplot for relative bed height of 5.08 cm with fines.

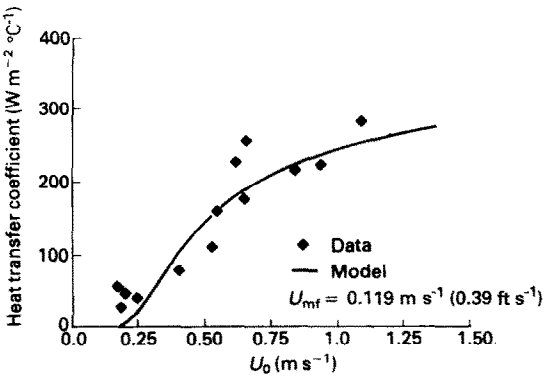

FIG. 17. Crossplot for relative bed height of 7.62 cm with fines.

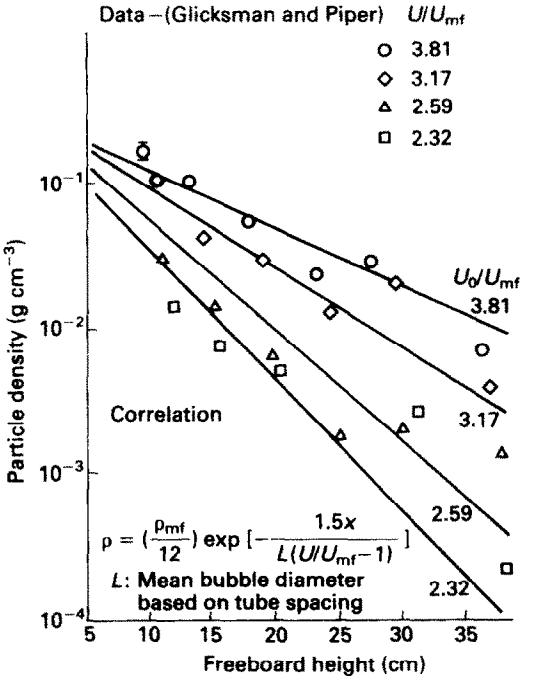

FIG. 18. Particle density vs freeboard height.

experimental value of $\bar{x}$. Comparison is only shown for the two largest sized particles that George and Grace [1] used; it is unclear if the 0.470 mm particle diameter qualifies as a large particle as assumed in the present model. Since most of their results are for the lowest row in a tube bank of four rows in the splash zone the assumption that the horizontal tube pitch is proportional to the bubble size in the bed and to the appropriate system dimension L in equation (10) is open to question.

Byam *et al.* [2] do not report the minimum fluidization velocity, particle sphericity or density. In this case U_{mf} was estimated from Wen and Yu's correlation with a particle density of 2400 kg m^{-3} which gave a $U_{mf} = 0.22$ m s^{-1}.

The results of Biyikli *et al.* and Xavier and Davidson were not used since most of their tests appeared to be in slug flow rather than bubbling flow.

Kortleven *et al.* present their data for range of velocities, an average velocity was used in the comparison in the table. Figure 19 shows a comparison of their results for different superficial velocities vs height above the expanded bed surface. The agreement is very close between the data and the proposed correlation.

CONCLUSIONS

Heat transfer to horizontal tubes in the splash zone of a bubbling fluidized bed decreases exponentially with the vertical distance above the expanded surface of the bed.

The data for six different banks of horizontal tubes is correlated by use of a nondimensional vertical distance, $xU_{mf}/L(U-U_{mf})$. For staggered tube arrays L is the horizontal pitch. Variations in the vertical tube pitch do not appreciably influence the heat transfer behavior in the splash zone although the vertical pitch does influence the rate of bed expansion.

The splash zone heat transfer correlation, derived from a simple model for large particle acceleration,

Table 2. Splash zone heat transfer for horizontal tube bundles. Comparison of correlation with other work

Reference	Particle diameter (m)	Bed temperature (K)	Pressure	U/U_{mf}	$\bar{x}$ (experimental) (cm)	$\bar{x}$ (equation (14)) (cm)
George and Grace	890	400	Atmospheric	3	20	11
	890			2	13	6
	470			8	21	33
	470			4.5	15	19
Byam *et al.*	860	1030 and 1060	6 bar	5.6[a]	20	27
Kortleven *et al.*	1100	1116–1150	Atmospheric	6.4 (Avg.)	46	43

Equation (14): $\bar{x} = \dfrac{L(U-U_{mf})}{1.5U_{mf}}$.

[a]Based on calculated value of U_{mf} (see text).

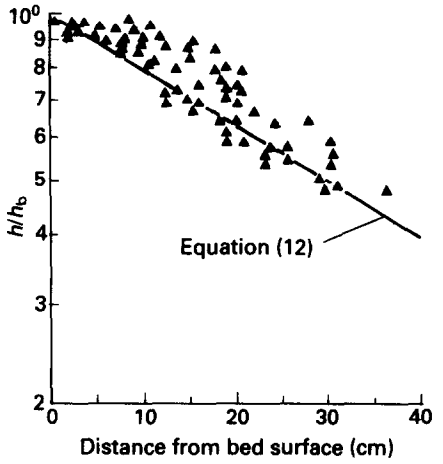

FIG. 19. Heat transfer coefficient in the splash zone. Data of Kortleven *et al.* compared to equation (12).

gives reasonable agreement with other data in the literature.

The splash zone heat transfer is proportional to the local particle density in the splash zone.

Acknowledgements—The research was carried out under sponsorship of the Tennessee Valley Authority; special thanks are due to Rick Carson of TVA. Some of the tests were carried out with the assistance of John Washington and Eric Glicksman.

REFERENCES

1. S. E. George and J. R. Grace, Heat transfer to horizontal tubes in the freeboard region of a gas fluidized bed, *A.I.Ch.E. Jl* **28,** 5 (1982).
2. J. Byam, K. K. Pillai and A. G. Roberts, Heat transfer to cooling coils in the splash zone of a pressurized fluidized bed combustor, *A.I.Ch.E. Symp. Series* **77**(208), 351 (1981).
3. A. Kortleven, J. Bast and J. Meulink, Heat transfer for horizontal tubes in the splash zone of a 0.6 × 0.6 m AFBC research facility, *Proc. XVIth Int. Center of Heat and Mass Transfer Conf.*, Yugoslavia (1984).
4. A. M. Xavier and J. F. Davidson, Heat transfer to surfaces immersed in fluidized beds and in the freeboard region, *A.I.Ch.E. Symp. Series* **77**(208), 368 (1981).
5. S. Biyikli, K. Tuzla and J. C. Chen, Heat transfer around a horizontal tube in the freeboard region of a fluidized bed, *A.I.Ch.E. Jl* **29,** 5 (1983).
6. R. T. Wood, M. Kuwata and F. W. Staub, Heat transfer to horizontal tube banks in the splash zone of a fluidized bed of large particles. In *Fluidization* (Edited by J. R. Grace and J. M. Matsen), p. 235. Plenum, New York (1980).
7. M. T. Nicastro and L. R. Glicksman, Experimental verification of scaling relationships for fluidized beds, *Chem. Engng Sci.* **39**(9), 1381–1391 (1984).
8. L. R. Glicksman, Scaling relationships for fluidized beds, *Chem. Engng Sci.* **39**(9), 1373–1379 (1984).
9. L. Jones and L. R. Glicksman, An experimental investigation of gas flow in a scale model of a fluidized-bed combustor, *Powder Technol.* **45**(3), 201–214 (February 1986).
10. W. L. Lewis, E. R. Gilliland and P. M. Lang, Entrainment from fluidized beds, *Chem. Engng Prog. Symp. Series* **38,** 58 (1962).
11. Glenn Alvah Piper III, A determination of particle density distribution above fluidized beds, M.S. Thesis in Mechanical Engineering, Massachusetts Institute of Technology, Cambridge, Massachusetts (May 1985).
12. L. R. Glicksman and T. Yule, Gas throughflow in a bubbling fluidized bed, *Proc. Fluidization V Conf.* (Edited by K. Østergaard), pp. 103–110. Elsinore, Denmark (May 1986).
13. E. K. Levy, J. C. Dille and H. S. Carem, Single particle eruptions in gas fluidized beds, *Powder Technol.* **32,** 173–178 (1982).
14. N. Decker and L. R. Glicksman, Heat transfer in large particle fluidized beds, *Int. J. Heat Mass Transfer* **26,** 1307–1320 (1983).

TRANSFERT THERMIQUE DANS LA ZONE D'ECLABOUSSEMENT D'UN LIT FLUIDISE A BULLES

Résumé—Le transfert thermique est mesuré dans la zone d'éclaboussement d'un lit fluidisé à bulles pour six géométries différentes de grappes de tubes horizontaux et dans un domaine de vitesses spécifiques. Le transfert thermique décroît exponentiellement avec la distance verticale au dessus de l'expansion de surface du lit. Les résultats sont corrélés en utilisant une distance verticale adimensionnelle $XU_{mf}/L(U-U_{mf})$ où L est le pas horizontal des tubes dans un arrangement étagé. La même corrélation donne un accord raisonnable avec d'autres données prises dans la littérature pour des lits à bulles avec larges particules. Le transfert thermique dans la zone d'éclaboussement est proportionnel à la densité locale particulaire mesurée dans cette zone.

WÄRMEÜBERGANG IN DER SPRITZZONE EINER BRODELNDEN WIRBELSCHICHT

Zusammenfassung—Es wird der Wärmeübergang in der Spritzzone einer brodelnden Wirbelschicht für sechs verschiedene Anordnungen horizontaler Rohrbündel gemessen. Der Wärmeübergang verringert sich exponentiell mit dem vertikalen Abstand über der erweiterten Bettoberfläche. Die Ergebnisse werden mit einem dimensionslosen vertikalen Abstand $XU_{mf}/L(U-U_{mf})$ korreliert, wobei L der horizontale Abstand der Rohre in einer versetzten Anordnung ist. Mit dieser Korrelation erhält man eine gute Übereinstimmung mit Werten aus der Literatur für Wirbelschichten mit großen Partikeln. Der Wärmeübergang in der Spritzzone ist proportional zur gemessenen lokalen Partikeldichte in der Spritzzone.

ТЕПЛОПЕРЕНОС В ЗОНЕ РАЗБРЫЗГИВАНИЯ ПУЗЫРЬКОВОГО ПСЕВДООЖИЖЕННОГО СЛОЯ

Аннотация—Определяется теплоперенос в зоне разбрызгивания пузырькового псевдоожиженного слоя при шести различных геометриях горизонтальных пучков труб для различных скоростей на поверхности. Величина теплопереноса экспоненциально уменьшается с ростом вертикального расстояния над поверхностью слоя. Результаты обобщаются с использованием безразмерного вертикального расстояния $XU_{mf}/L(U - U_{mf})$, где L—горизонтальный интервал между трубами, расположенными в махматном поредке. Полученное соотношение удовлетворительно согласуется с другими имеющимися в литературе данными для пузырьковых слоев крупных частиц. Величина теплопереноса в зоне разбрызгивания пропорциональна измеренной локальной плотности частиц.